Decreased iPLA$_2\gamma$ expression induces lipid peroxidation and cell death and sensitizes cells to oxidant-induced apoptosis

Gilbert R. Kinsey,[1,*] Jason L. Blum,[1,*] Marisa D. Covington,[*] Brian S. Cummings,[†] Jane McHowat,[§] and Rick G. Schnellmann[2,*]

Department of Pharmaceutical and Biomedical Sciences and Center for Cell Death, Injury, and Regeneration,* South Carolina College of Pharmacy, Medical University of South Carolina, Charleston, SC 29425; Department of Pharmaceutical and Biomedical Sciences,[†] University of Georgia, Athens, GA 30602; and Department of Pathology,[§] St. Louis University, St. Louis, MO 63104

Abstract **Our previous studies showed that renal proximal tubular cells (RPTC) express Ca^{2+}-independent phospholipase $A_2\gamma$ (iPLA$_2\gamma$) in endoplasmic reticulum (ER) and mitochondria and that iPLA$_2\gamma$ prevents and/or repairs lipid peroxidation induced by oxidative stress. Our present studies determined the importance of iPLA$_2\gamma$ in mitochondrial and cell function using an iPLA$_2\gamma$-specific small hairpin ribonucleic acid (shRNA) adenovirus. iPLA$_2\gamma$ expression and activity were decreased in the ER by 24 h and in the mitochondria by 48 h compared with scrambled shRNA adenovirus-treated cells. Lipid peroxidation was elevated by 2-fold at 24 h and remained elevated through 72 h in cells with decreased iPLA$_2\gamma$. Using electrospray ionization-mass spectrometry, primarily phosphatidylcholines and phosphatidylethanolamines were increased in iPLA$_2\gamma$-shRNA-treated cells. At 48 h after exposure to the iPLA$_2\gamma$ shRNA, uncoupled oxygen consumption was inhibited by 25% and apoptosis was observed at 72 and 96 h. RPTC with decreased iPLA$_2\gamma$ expression underwent apoptosis when exposed to a nonlethal concentration of the oxidant *tert*-butyl hydroperoxide (TBHP). Exposure of control cells to a nonlethal concentration of TBHP induced iPLA$_2\gamma$ expression in RPTC. These results suggest that iPLA$_2\gamma$ is required for the prevention and repair of basal lipid peroxidation and the maintenance of mitochondrial function and viability, providing further evidence for a cytoprotective role for iPLA$_2\gamma$ from oxidative stress.—** Kinsey, G. R., J. L. Blum, M. D. Covington, B. S. Cummings, J. McHowat, and R. G. Schnellmann. **Decreased iPLA$_2\gamma$ expression induces lipid peroxidation and cell death and sensitizes cells to oxidant-induced apoptosis. *J. Lipid Res.* 2008.** 49: **1477–1487.**

Supplementary key words Ca^{2+}-independent phospholipase A_2 • renal proximal tubular cells • mitochondria

Phospholipase A_2 (PLA_2) hydrolyzes the *sn*-2 ester bond of glycerophospholipids. By this mechanism, PLA_2 generates free fatty acids and lysophospholipids, both of which have biological activity. The family of PLA_2 is large, with >20 isoforms that were separated historically into classes based on Ca^{2+} requirement or localization [cytosolic, secretory, or Ca^{2+}-independent PLA_2 (iPLA$_2$)] and recently into 15 groups based on amino acids utilized for catalysis and other structural and functional similarities (groups I–XV) (1). The iPLA$_2$ family consists of at least seven members, with different isoforms being localized to different subcellular compartments, each displaying PLA_2 activity in the absence of Ca^{2+} (1).

PLA_2 is reported to perform diverse functions, including generation of signaling molecules [e.g., arachidonic acid (2), membrane remodeling (3), and protection or repair of membranes from oxidative damage (4–6)]. In support of a protective role for PLA_2, PLA_2 has been hypothesized to participate in the removal of oxidized fatty acids from biological membranes to maintain membrane integrity (7). Fatty acids at the *sn*-2 position of glycerophospholipids

This research was supported by National Institutes of Health Grant DK-62028 to R.G.S. G.R.K. was supported by a training grant from the National Institute of Environmental Health Sciences, National Institutes of Health (Grant T32 ES-012878), and J.L.B. was supported by an individual National Institutes of Health National Research Service Award training fellowship (Grant F32 DK-081267). The Medical University of South Carolina animal facilities were funded by National Institutes of Health Grant C06 RR-015455. The data presented here are solely the responsibility of the authors and do not represent the official views of the National Institutes of Health.

Manuscript received 15 June 2007 and in revised form 16 January 2008 and in re-revised form 4 March 2008 and in re-re-revised form 7 April 2008.

Published, JLR Papers in Press, April 8, 2008.
DOI 10.1194/jlr.M800030-JLR200

Abbreviations: BEL, bromoenol lactone; DAPI, 4′,6-diamidino-2-phenylindole; ER, endoplasmic reticulum; FCCP, carbonyl cyanide *p*-(trifluoromethoxy) phenylhydrazone; iPLA$_2$, Ca^{2+}-independent phospholipase A_2; MPT, mitochondrial permeability transition; PI, propidium iodide; PLA_2, phospholipase A_2; QO_2, oxygen consumption; RCM, renal cortex mitochondria; RPTC, renal proximal tubular cell; TBARS, thiobarbituric acid-reactive substances; TBHP, *tert*-butyl hydroperoxide.

[1] G. R. Kinsey and J. L. Blum contributed equally to this work.
[2] To whom correspondence should be addressed.
e-mail: schnell@musc.edu

are preferred targets of reactive oxygen species due to their relatively high degree of unsaturation. van Kuijk et al. (7) proposed that when lipid peroxidation occurs, the oxidized *sn*-2 fatty acid of phospholipids becomes less hydrophobic and moves closer to the hydrophilic head of the phospholipid. The movement of this fatty acid increases the space between the polar head groups and exposes the *sn*-2 ester bond to PLA_2. This phenomenon would result in an apparent preference of certain PLA_2s for oxidized phospholipids. The cleavage of oxidized fatty acids releases a lysophospholipid, which can be reacylated with a nonoxidized fatty acid by an acyltransferase and reinserted into the membrane, preserving membrane integrity (8). The oxidized fatty acids can be detoxified through classical glutathione peroxidases, but only after they are released by the action of PLA_2 (9, 10). Secretory PLA_2 and cytosolic PLA_2 have been used in vitro to test the hypothesis that PLA_2 can act as repair enzymes in synthetic membranes or isolated microsomes (11, 12), but the native PLA_2 enzyme(s) responsible for the repair of oxidized phospholipids in intact cellular systems has not been identified.

Two members of the $iPLA_2$ family, $iPLA_2\beta$ and $iPLA_2\gamma$ (groups VIA and VIB, respectively), are reported to protect cells or organelles during oxidative stress (4–6). Overexpression of $iPLA_2\beta$ in insulinoma cells and CHO cells results in mitochondrial localization of $iPLA_2\beta$ and protects against oxidant-induced apoptosis (6). In primary cultures of rabbit renal proximal tubule cells (RPTCs), inhibition of $iPLA_2\gamma$ with racemic bromoenol lactone (BEL) potentiated oxidant-induced lipid peroxidation and necrotic cell death (4). Furthermore, in isolated rabbit renal cortex mitochondria (RCM), pretreatment with the selective $iPLA_2\gamma$ inhibitor R-BEL (the *R*-enantiomer of BEL) accelerated Fe^{2+}-induced lipid peroxidation and mitochondrial swelling (5). In summary, several studies have reported that $iPLA_2$ enzymes are important mediators of cell and organelle protection from oxidative stress and lipid peroxidation.

The goal of these experiments was to determine the importance of $iPLA_2\gamma$ in basal mitochondrial and cellular function. Since previous results from our laboratory suggested that the $iPLA_2\gamma$ isoform protects renal cells and mitochondria from oxidative damage (4, 5), we hypothesized that decreasing $iPLA_2\gamma$ expression in RPTC would increase lipid peroxidation, impair mitochondrial function, and decrease viability. To test this hypothesis, RPTCs were infected with adenovirus expressing small hairpin ribonucleic acid (shRNA) to decrease the expression of $iPLA_2\gamma$. We also examined the sensitivity of these cells to the model oxidant *tert*-butyl hydroperoxide (TBHP).

EXPERIMENTAL PROCEDURES

Materials

Annexin V-FITC was purchased from Biovision (Mountain View, CA). All other reagents were from Sigma (St. Louis, MO) or reported previously (13, 14).

Development of the $iPLA_2\gamma$ shRNA adenovirus

An shRNA insert corresponding to the $iPLA_2\gamma$ small interfering RNA (sense strand, 5′-gcaagcaacuguauuucuutt-3′; Ambion, Austin, TX) was designed using the Insert Design Tool for pSilencer Vectors on the Ambion website (www.ambion.com). This oligonucleotide was used to generate an adenoviral $iPLA_2\gamma$ shRNA vector using the pSilencer Adeno-CMV system (Ambion) according to the manufacturer's protocol. The crude viral lysate was then transferred to the Viral Vector Core Facility at the Medical University of South Carolina for amplification, purification, and titer determination. The negative control adenovirus, Ad-CMV-RNAi, was obtained from Vector Biolabs (Philadelphia, PA).

Isolation of rabbit RPTCs, culture conditions, and adenovirus treatment

Rabbit RPTCs were isolated using the iron oxide perfusion method and grown in 35 mm tissue culture dishes under improved conditions as described previously (15). Confluent monolayers were exposed to either the $iPLA_2\gamma$ shRNA adenovirus or a negative control scramble shRNA adenovirus at a concentration of 1×10^7 plaque-forming units per 35 mm dish for 24 h. After 24 h, the culture medium was changed to normal culture medium and the cells were cultured routinely and processed as described below.

Immunoblot analysis

Immunoblot analysis of the expression of 88 kDa $iPLA_2\gamma$ in RPTC mitochondrial and endoplasmic reticulum (ER) fractions was performed using an anti-$iPLA_2\gamma$ antibody as described previously by our laboratory (5). Heat shock protein 60 was used as a mitochondrial marker and loading control for mitochondrial samples.

Measurement of $iPLA_2$ activity

PLA_2 activity was determined under linear reaction conditions in RPTC mitochondrial and ER fractions as described previously (5). Activity was measured using synthetic (16:0, [^{3}H]20:4) plasmenylcholine (100 μM) in the presence of 4 mM EGTA.

Measurement of apoptosis

Annexin V and propidium iodide (PI) staining were determined using flow cytometry as described previously by our laboratory (16). RPTCs were washed, fixed, and stained with 4′,6-diamidino-2-phenylindole (DAPI) as described previously (16). At least 200 nuclei were counted for each treatment group in each experiment.

Measurement of oxygen consumption

RPTC monolayers were washed and gently detached from the dishes with a rubber policeman, suspended in 37°C culture medium, and transferred to the oxygen consumption (QO_2) measurement chamber. QO_2 was measured polarographically using a Clark-type electrode as described previously (14, 17). For measurement of uncoupled QO_2, 1 μM carbonyl cyanide *p*-(trifluoromethoxy) phenylhydrazone (FCCP) was used.

Measurement of cellular ATP levels

Intracellular ATP levels were measured using the ATP Bioluminescence Assay Kit CLS II (Roche) as described previously (18).

Measurement of lipid peroxidation

Lipid peroxidation in RPTCs was monitored as the production of malondialdehyde using thiobarbituric acid-reactive substances (TBARS) as described previously (4).

Measurement of cellular phospholipids by electrospray ionization-mass spectrometry

At the end of the experimental period, culture media were removed from the dishes, the monolayers were rinsed with 1 ml of phosphate-buffered saline, and the cells were scraped into 1 ml of methanol-water (2.5:1). RPTCs from four dishes were pooled for each experiment. Whole cells were used to identify lipid changes because of the likelihood of lipid mixing during mitochondrial isolation. The cell suspension was then transferred to a glass vial, bubbled extensively with nitrogen, and stored at −80°C until extraction.

Lipids were isolated using a modified method of Bligh and Dyer (19) as described by Zhang, Peterson, and Cummings (20). Following extraction, the samples were evaporated under a stream of argon gas to near dryness. The lipids were then reconstituted in 95 μl of chloroform-methanol (2:1) and 5 μl of 1 mg/ml deuterated palmitate (m/z 259.5) in chloroform-methanol (2:1), as an internal standard for ESI-MS. Total lipid phosphorus was measured in each sample using malachite green (21), and the samples were diluted to 5 nmol/ml total lipid phosphorus in chloroform-methanol (2:1). ESI-MS was performed as described previously (20) using a Trap XCT ion-trap mass spectrometer (Agilent Technologies, Santa Clara, CA) with a nitrogen-drying gas flow rate of 3 l/min at 300°C and a nebulizer pressure of 10 p.s.i. The scanning range was from 100 to 2,200 m/z on 5 μl of sample scanned for 2.5 min with a mobile phase of acetonitrile-methanol-water (2:3:1) in 0.1% ammonium formate. Phospholipids were analyzed in both positive and negative ion detection modes.

Statistical analysis

Each experiment was performed using RPTCs from a single rabbit and was repeated at least four times. The appropriate ANOVA was performed for each data set using SigmaStat statistical software. Individual means were compared using Fisher's protected least significant difference test with $P < 0.05$ considered indicative of a statistically significant difference among mean values.

To analyze the mass spectrometry data, the m/z peaks were sorted by m/z and aligned to a master list compiled from the Lipid Maps Consortium (www.lipidmaps.org). Values from Lipid Maps were increased by one for positive mode and decreased by one in negative mode. The negative ion mode spectra were first normalized to the deuterated palmitate peak and then, using the central limit theorem, transformed as described previously (22, 23). Data from the positive mode were first normalized to the mean values of all of the samples and then transformed using the central limit theorem transformation method. After data normalization, the data were analyzed using ANOVA, and when significant effects were found ($P < 0.05$), individual means were compared using Duncan's multiple range test ($\alpha = 0.05$). The only comparisons that were considered meaningful were when iPLA$_2\gamma$ shRNA (24 or 48 h) treatments were significantly different from uninfected control and scrambled shRNA (24 or 48 h).

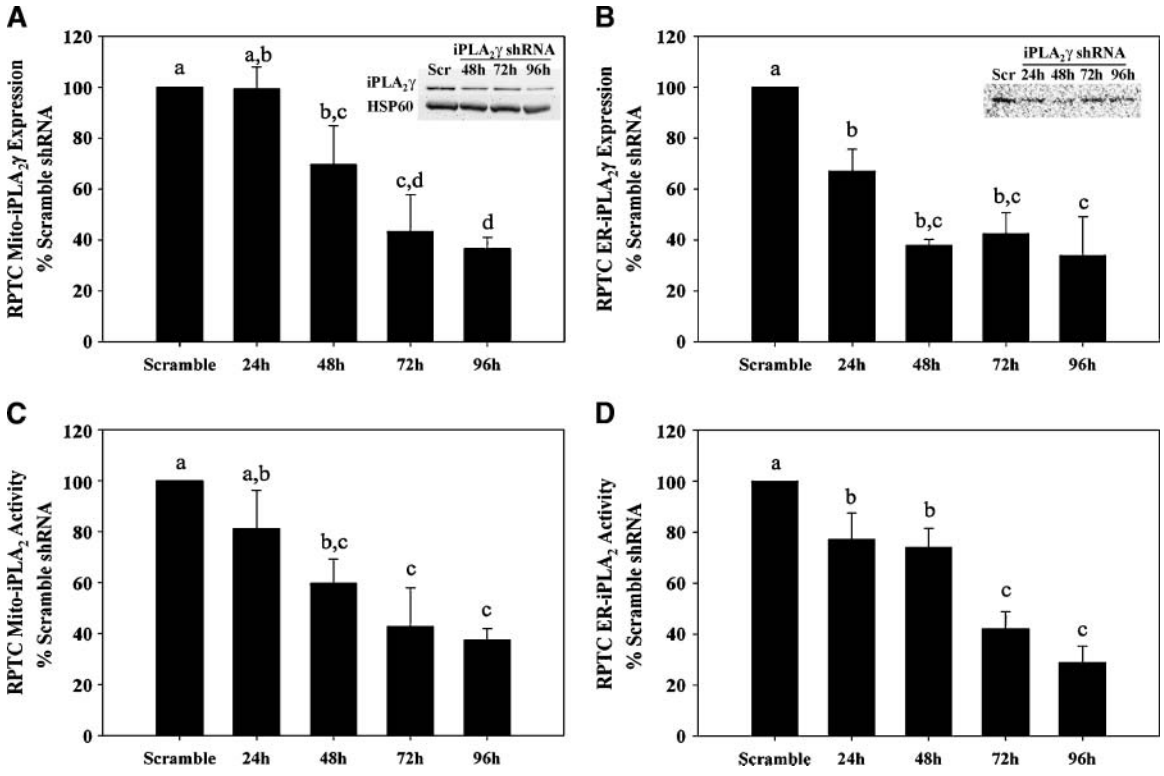

Fig. 1. Small hairpin ribonucleic acid (shRNA)-mediated decreases in mitochondrial and endoplasmic reticulum (ER) Ca^{2+}-independent phospholipase A_2 (iPLA$_2\gamma$) in rabbit renal proximal tubular cells (RPTCs). Confluent RPTCs were exposed to either adenoviral iPLA$_2\gamma$ or scramble shRNA and cultured normally for 4 days. iPLA$_2\gamma$ expression was measured by immunoblot analysis (A, B) and iPLA$_2$ activity was measured as described in Experimental Procedures (C, D) in mitochondrial (A, C) and ER (B, D) fractions at 24, 48, 72, and 96 h after exposure. The amount of iPLA$_2\gamma$ expression and activity in cells exposed to iPLA$_2\gamma$ shRNA is expressed as means + SEM, percentage of iPLA$_2\gamma$ expression and activity in cells exposed to scramble shRNA for the same amount of time. Insets show representative immunoblots. Means with different superscripts are significantly different from each other ($P < 0.05$, n = 4–5).

RESULTS

Adenoviral shRNA-mediated knock-down of RPTC iPLA$_2$γ

Infection of RPTCs with the iPLA$_2$γ shRNA adenovirus resulted in ~80% of cells expressing the transgene, as determined by β-galactosidase staining (data not shown). Mitochondrial iPLA$_2$γ protein expression and activity were reduced by ~40% at 48 h after iPLA$_2$γ shRNA adenovirus treatment compared with RPTCs exposed to an equivalent amount of scramble shRNA adenovirus (**Fig. 1A, C**). Mitochondrial iPLA$_2$γ protein and activity levels continued to decrease to ~40% of scramble shRNA-treated cell values at 72 and 96 h. No significant changes in expression or activity of iPLA$_2$γ in noninfected control cells and scramble shRNA adenovirus-treated cells were observed (data not shown). In contrast, protein levels of iPLA$_2$γ in the ER fraction of RPTC decreased after 24 h (~65% of scramble shRNA) and decreased to ~40% of scramble shRNA at 48, 72, and 96 h after exposure to iPLA$_2$γ shRNA (Fig. 1B). ER-iPLA$_2$γ activity was also decreased (~25%) at 24 h after exposure to the iPLA$_2$γ shRNA adenovirus, and activity decreased to ~35% of scramble shRNA at 72 and 96 h (Fig. 1D). In summary, adenovirus-mediated knock-down of iPLA$_2$γ protein levels and activity occurred in the ER fraction prior to occurring in the mitochondria, but it resulted in similar decreases (60–70%) in both organelles by 72 h.

Knock-down of RPTC iPLA$_2$γ causes increases in RPTC phospholipids

We determined the effect of iPLA$_2$γ knock-down on RPTC phospholipids. A total of 267 *m/z* values were examined for the phospholipids in each ion mode. Of these, one positive and nine negative *m/z* species were putatively identified as being specifically increased by decreasing the expression of iPLA$_2$γ (**Table 1**). The single positive phospholipid that increased was *m/z* 865 [42:5 (*sn*-1 + *sn*-2) phosphatidylcholine (PC), 36:1 phosphatidylinositol (PI), or 43:6 phosphatidylglycerol (PG)] after 24 h, which returned to control levels by 48 h. For the negative phospholipids, four *m/z* species were increased by 24 h {578 [24:0 phosphatidylethanolamine (PE)], 730 [32:2 phosphatidylserine (PS)], 795 [31:1 PI or 38:5 PG], and 985 [40:8 PI phosphate]}, while five *m/z* species were elevated by 48 h [693 (30:0 PG), 725 (26:0 PI or 33:5 PG), 844 (40:1 PS, 40:0 PC, or 44:7 PE), 860 (41:0 PS, 42:7 PS, or 42:6 PC), and 873 (37:3 PI, 43:1 PG, 44:8 PG)]. Specific identification of these phospholipid species will require tandem MS^n to identify exactly which they are. In summary, ablation of 60% of cellular iPLA$_2$γ resulted in the increase of several specific cellular phospholipids of the phosphatidylcholine, phosphatidylethanolamine, and phosphatidylglycerol classes.

Knock-down of iPLA$_2$γ increases RPTC lipid peroxidation

Previous studies from our laboratory demonstrated that inhibition of iPLA$_2$γ led to increased oxidant-induced lipid peroxidation in RPTCs (4) and in isolated renal mito-

TABLE 1. Phospholipids increased by knock-down of iPLA$_2$γ in RPTCs

Positive mode phospholipids	[M+H]									
	865									
Control	−0.52 ± 0.41^a									
shRNA, 24 h	**1.26 ± 0.38^b**									
shRNA, 48 h	−0.17 ± 0.52^a									
Scrambled, 24 h	−0.17 ± 0.24^a									
Scrambled, 48 h	−0.55 ± 0.13^a									
Negative mode phospholipids	[M-H]									
	578	693	725	730	795	844	860	873	985	
Control	−0.27 ± 0.13^a	−0.37 ± 0.07^a	−0.23 ± 0.13^a	−0.31 ± 0.07^a	−0.36 ± 0.07^a	−0.23 ± 0.14^a	−0.29 ± 0.19^a	−0.38 ± 0.03^a	−0.21 ± 0.06^a	
shRNA, 24 h	**1.31 ± 1.01^b**	−0.35 ± 0.13^a	−0.25 ± 0.13^a	**1.18 ± 0.92^b**	**1.16 ± 0.94^b**	−0.30 ± 0.16^a	−0.49 ± 0.32^a	0.09 ± 0.29^{ab}	**1.32 ± 1.09^b**	
shRNA, 48 h	−0.33 ± 0.07^a	**1.27 ± 0.75^b**	**1.18 ± 0.81^b**	−0.27 ± 0.15^a	−0.38 ± 0.12^a	**1.15 ± 0.80^b**	**1.21 ± 0.61^b**	**1.05 ± 0.84^b**	−0.32 ± 0.00^a	
Scrambled, 24 h	−0.40 ± 0.00^a	−0.31 ± 0.20^a	−0.39 ± 0.12^a	−0.46 ± 0.08^a	−0.46 ± 0.11^a	−0.24 ± 0.19^a	−0.02 ± 0.23^a	−0.39 ± 0.07^a	−0.20 ± 0.11^a	
Scrambled, 48 h	−0.05 ± 0.30^a	−0.36 ± 0.07^a	−0.53 ± 0.03^a	−0.45 ± 0.13^a	−0.50 ± 0.35^a	−0.35 ± 0.10^a	−0.32 ± 0.00^a			

iPLA$_2$, Ca^{2+}-independent phospholipase A_2; [M−H], loss of a proton; [M+H], gain of a proton; small hairpin ribonucleic acid, shRNA; RPTC, renal proximal tubular cell. iPLA$_2$γ was knocked down in RPTCs and whole cell lipids were isolated using a modified Bligh and Dyer (19) method. Phospholipids were identified using ESI-MS in both positive and negative ion modes. Data were normalized using the central limit theorem as described in Experimental Procedures and are presented as means ± SEM from four or five different rabbits. Within lipid species, means with the same letters were not significantly different as determined by Duncan's multiple range test. Where SEM is equal to zero, the particular lipid species was not identified by ESI-MS in any of the samples from that treatment. Boldface values are statistically significant within that particular phospholipid.

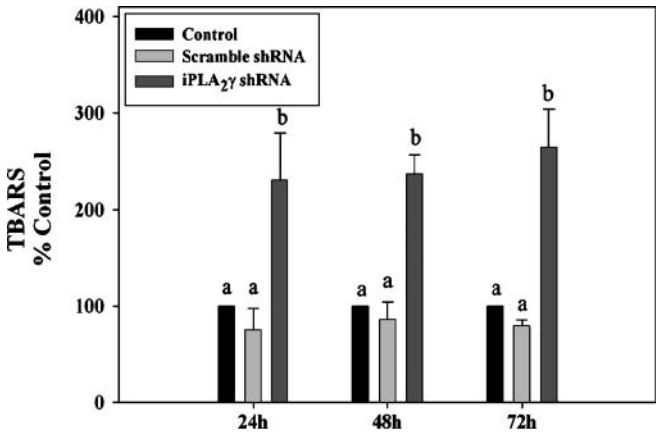

Fig. 2. Effects of decreased iPLA$_2$γ expression on RPTC lipid peroxidation. The thiobarbituric acid-reactive substances (TBARS) assay was performed in noninfected (control), scramble shRNA, and iPLA$_2$γ shRNA adenovirus-treated RPTCs at 24, 48, and 72 h after virus exposure as a measure of cellular lipid peroxidation. Data are presented as means + SEM, percentage of control TBARS formation. Means with different superscripts are significantly different from each other ($P < 0.05$, n = 4).

chondria (5). Accordingly, RPTC lipid peroxidation was measured in RPTCs after exposure to the scramble or iPLA$_2$γ shRNA adenovirus or diluent (control) using the TBARS assay (**Fig. 2**). Lipid peroxidation was elevated by ~2-fold at 24 h after exposure to the iPLA$_2$γ shRNA adenovirus compared with control or scramble shRNA adenovirus (Fig. 2). TBARS remained elevated by 2-fold above control through 72 h. These results indicate that knocking down iPLA$_2$γ in RPTCs increases lipid peroxidation prior to the onset of cell death.

Knock-down of RPTC iPLA$_2$γ causes changes in cellular and nuclear morphology and apoptosis

Light microscopy revealed that knock-down of iPLA$_2$γ resulted in RPTC cell death at 72 and 96 h (**Fig. 3**). No toxicity was observed through 96 h in control cells (data not shown) or RPTCs exposed to the scramble shRNA adenovirus (Fig. 3). The cell death observed consisted of RPTC shrinkage and detachment of cells from the plate. Examination of control (data not shown) and scramble shRNA-treated RPTC nuclear morphology, using the nuclear stain DAPI, revealed diffuse nuclear staining consistent with healthy RPTC. In contrast, 72 and 96 h after iPLA$_2$γ shRNA exposure, RPTC nuclei were condensed (15–20%) or fragmented (4–6%) (Figs. 3, 4).

Annexin V-FITC and PI staining coupled with flow cytometry was used as an additional marker of apoptosis after knock-down of iPLA$_2$γ in RPTC. Annexin V-FITC binds to externalized phosphatidyserine on apoptotic cells, while PI stains the DNA of necrotic cells. Beginning at 72 h after iPLA$_2$γ shRNA adenovirus exposure and persisting at 96 h, annexin V staining increased compared with control or scramble shRNA-treated RPTCs (**Fig. 4C**). No increases in PI staining were detected in any treatment group at any time point (data not shown). In summary, the data reveal that knock-down of iPLA$_2$γ in RPTCs results in apoptotic cell death.

Knock-down of RPTC iPLA$_2$γ inhibits RPTC mitochondrial function

To determine the effect of decreasing iPLA$_2$γ expression on mitochondrial function in RPTCs, basal and uncoupled QO_2 rates and ATP levels were determined. Uncoupled QO_2 is a measure of the maximum rate that electrons can be shuttled through the electron transport chain. A 25% decrease in basal QO_2 was observed at 96 h after iPLA$_2$γ shRNA adenovirus exposure compared with scramble shRNA treatment (**Fig. 5A**). Uncoupled QO_2 was inhibited by 25% after 48 h and remained inhibited through 96 h in RPTCs with decreased iPLA$_2$γ expression (Fig. 5B). No significant changes in basal or uncoupled QO_2 were observed in control or scramble shRNA-treated RPTCs over 96 h (data not shown). Similar

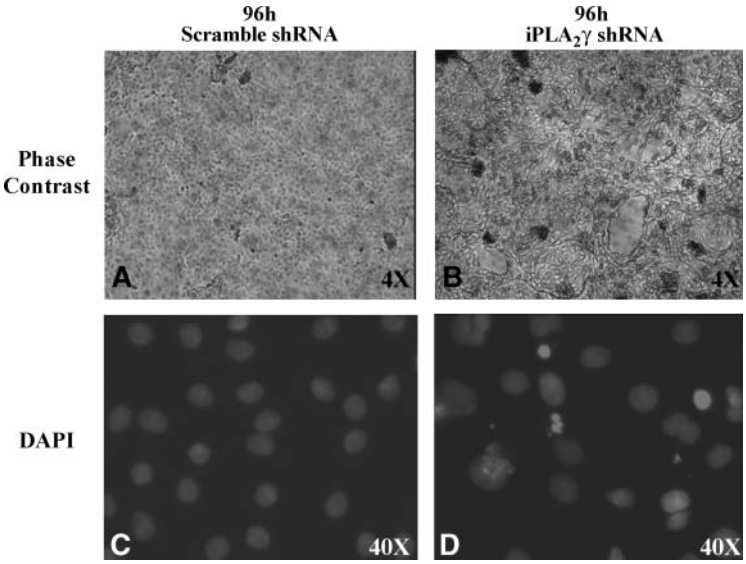

Fig. 3. Effects of decreased iPLA$_2$γ expression on cell and nuclear morphology in RPTCs. Confluent RPTCs were exposed to either adenoviral iPLA$_2$γ or scramble shRNA and cultured normally for 96 h. Representative photomicrographs are shown for cell (A, B) and nuclear (C, D) morphology in RPTCs at 96 h after exposure to scramble shRNA adenovirus (A, C) and iPLA$_2$γ shRNA adenovirus (B, D). Cells were fixed and stained with the nuclear dye, 4′,6-diamidino-2-phenylindole (DAPI) to assess nuclear morphology. Photomicrographs are representative of four separate RPTC preparations.

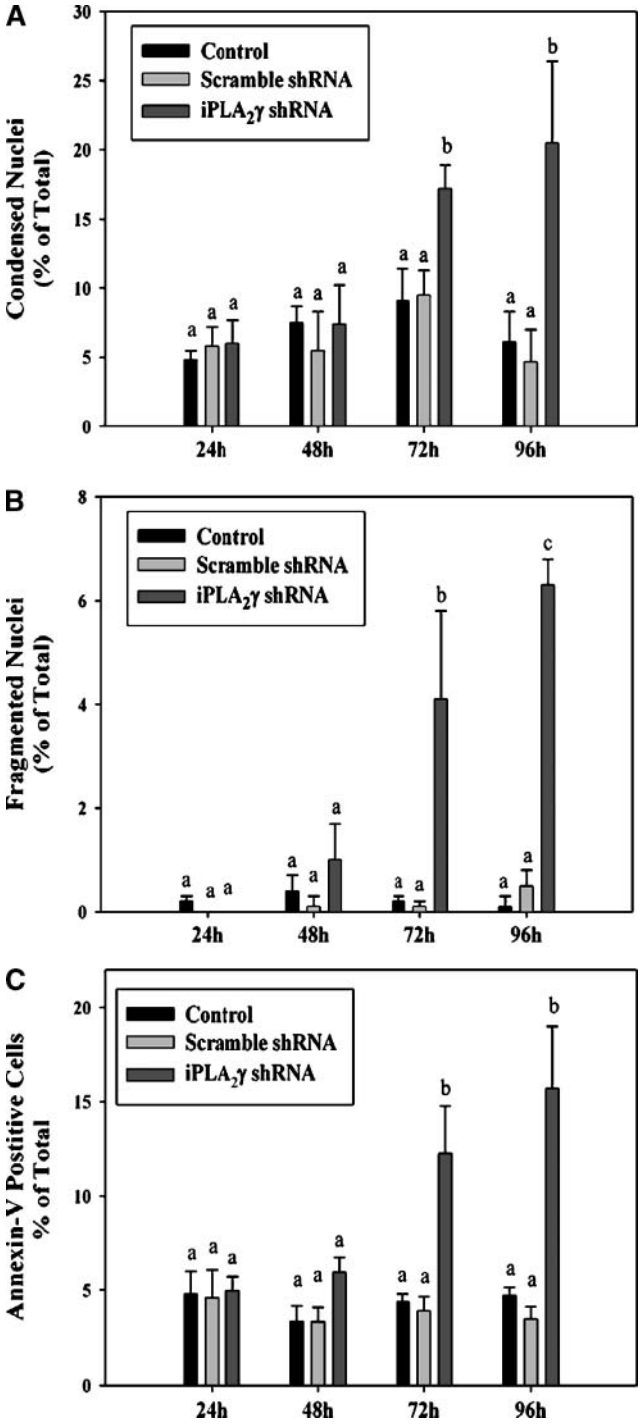

Fig. 4. Characterization of cell death induced by decreasing $iPLA_2\gamma$ expression. The percentage of cells with condensed or fragmented nuclei and cells with externalized phosphatidylserine was estimated by counting 10 high-power fields (per treatment group and per experiment) of DAPI-stained nuclei (A, B) and by flow cytometry of cells stained with annexin V-FITC and propidium iodide (PI) as described in Experimental Procedures (C) in noninfected (control), scramble shRNA, and $iPLA_2\gamma$ shRNA adenovirus-treated RPTCs at 24, 48, 72, and 96 h after virus exposure. Data are presented as means + SEM, percentage of total nuclei that displayed condensed or fragmented morphology (A, B) or annexin V staining in the absence of PI staining (C). Means with different superscripts are significantly different from each other ($P < 0.05$, n = 3–4).

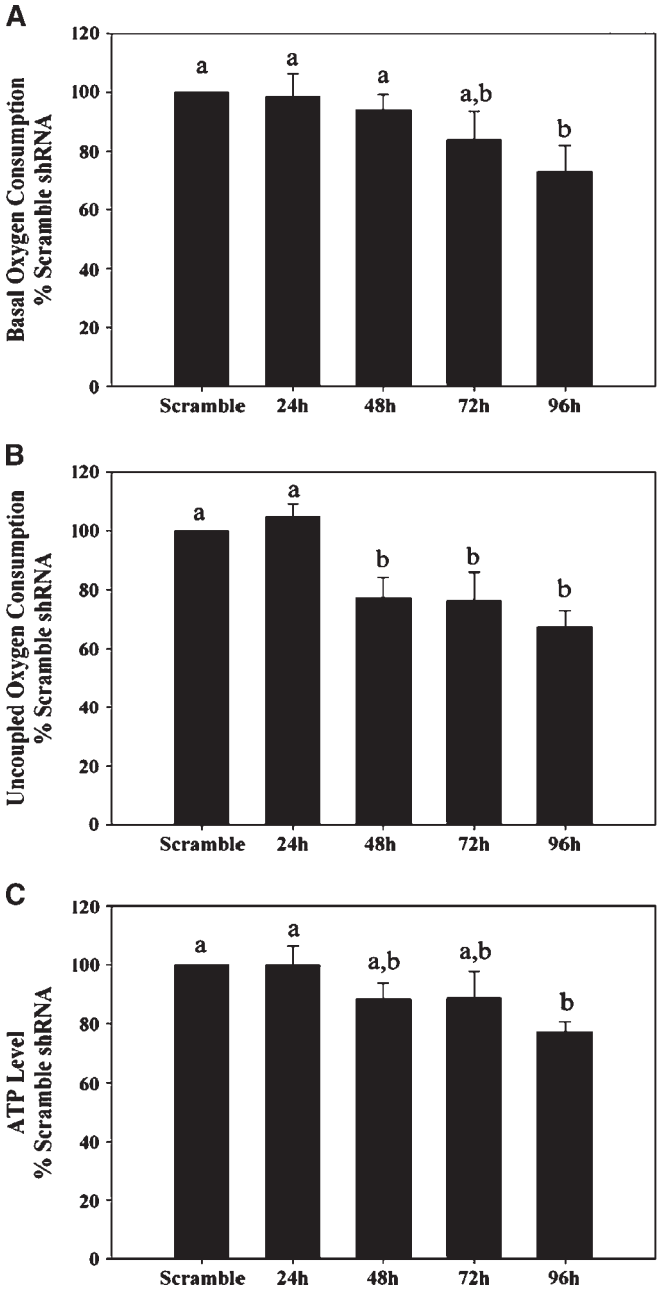

Fig. 5. Effects of decreased $iPLA_2\gamma$ expression on RPTC mitochondrial function. Basal (A) and uncoupled (B) oxygen consumption (QO_2) and cellular ATP levels (C) were measured in scramble shRNA and $iPLA_2\gamma$ shRNA adenovirus-treated RPTCs at 24, 48, 72, and 96 h after virus exposure. The rate of QO_2 or ATP level in cells exposed to $iPLA_2\gamma$ shRNA is expressed as means + SEM, percentage of cells exposed to scramble shRNA for the same amount of time. No differences in QO_2 or ATP levels between control RPTCs and scramble shRNA-treated RPTCs were detected at any time point. Means with different superscripts are significantly different from each other ($P < 0.05$, n = 4–5).

to basal QO_2, cellular ATP levels were reduced at 96 h after $iPLA_2\gamma$ shRNA exposure (Fig. 5C).

ER and mitochondrial $iPLA_2$ activity measurements were correlated with basal mitochondrial QO_2 (**Fig. 6A, E**). Uncoupled QO_2 was well correlated over time only with

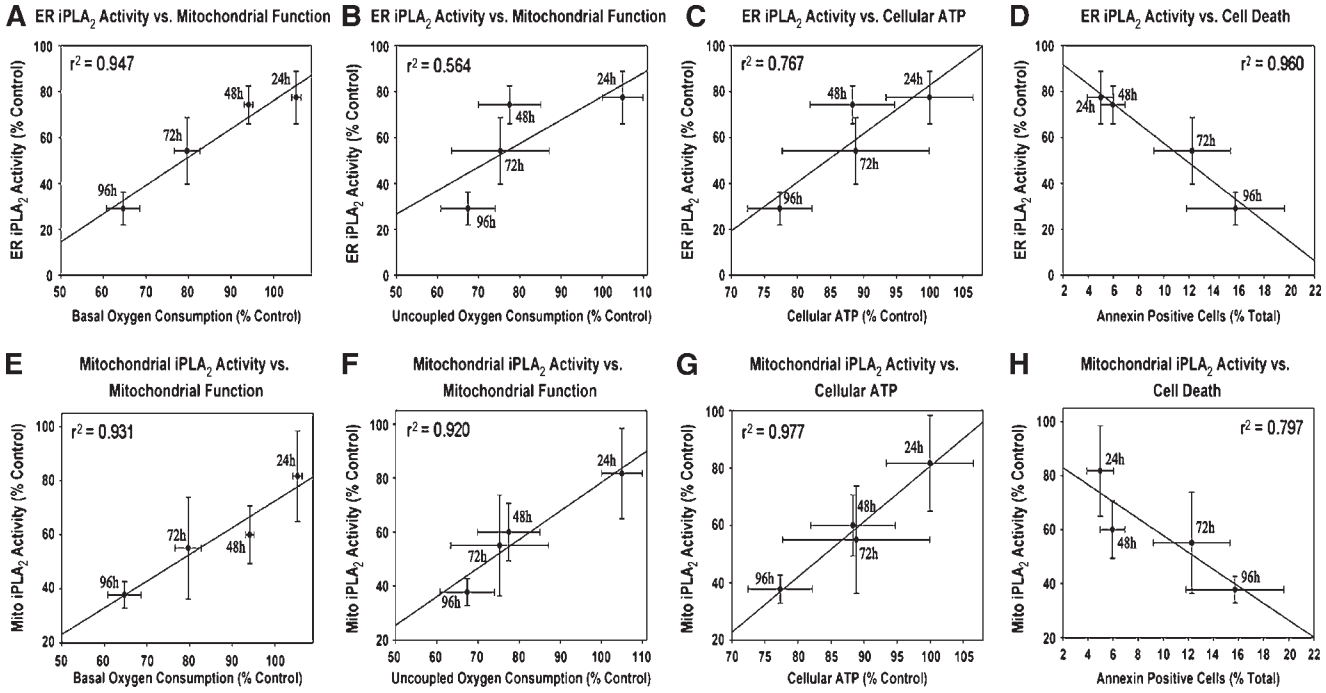

Fig. 6. Correlation of RPTC iPLA$_2$ activity with mitochondrial function and cell viability. Shown are iPLA$_2$ activity in ER (A–D) and mitochondria (E–H) isolated from RPTCs and basal (A, E) and uncoupled (B, F) QO_2, cellular ATP levels (C, G), and percentage of cells staining positive for annexin V-FITC and negative for PI (D, H) at the indicated time points after iPLA$_2\gamma$ shRNA adenovirus exposure. Data are reported as means ± SEM, percentage of scramble shRNA-treated control RPTC ER or mitochondrial iPLA$_2$ activity, QO_2, ATP levels, and annexin V-positive cells from the same time point.

mitochondrial iPLA$_2$ activity but not with ER iPLA$_2$ activity ($r^2 = 0.920$ vs. 0.564, respectively; Fig. 6B, F). The high correlation between uncoupled QO_2 and mitochondrial PLA$_2$ activity is consistent with the strong correlation between ATP levels and mitochondrial iPLA$_2\gamma$ activity (Fig. 6C, G). Both ER and mitochondrial iPLA$_2$ activity measurements were correlated with the percentage of apoptotic cells after exposure to the iPLA$_2\gamma$ shRNA adenovirus (Fig. 6D, H), suggesting that RPTC iPLA$_2\gamma$ activity is required for cell viability.

Apoptosis is induced by a nonlethal concentration of TBHP in RPTCs with decreased iPLA$_2\gamma$ expression

To determine the effect of iPLA$_2\gamma$ knock-down on sublethal oxidant stress, RPTCs with decreased iPLA$_2\gamma$, either in the ER fraction only (at 24 h after infection) or in

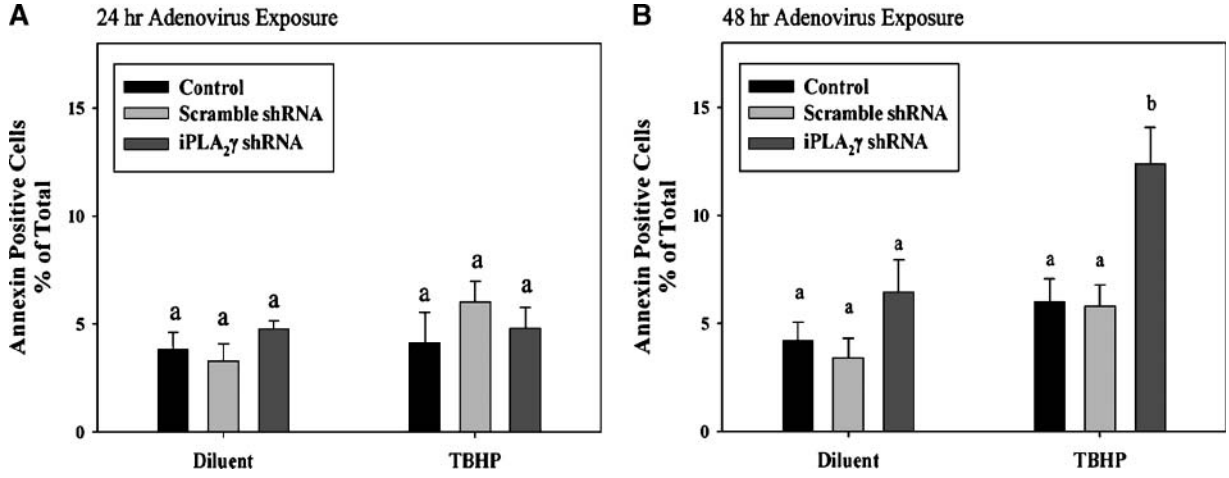

Fig. 7. Effects of decreased iPLA$_2\gamma$ expression on oxidant-induced apoptosis in RPTCs. After 24 h (A) and 48 h (B) of exposure to diluent (control), scramble shRNA, or iPLA$_2\gamma$ shRNA adenovirus, RPTCs were treated with *tert*-butyl hydroperoxide (TBHP; 75 μM) or diluent for 3 h and cell death was measured by flow cytometry after annexin V-FITC and PI staining. No significant changes in PI staining were detected in any group at any time point. Data are presented as means ± SEM; percentage of total cells analyzed that displayed annexin V staining in the absence of PI staining. Means with different superscripts are significantly different from each other ($P < 0.05$, n = 3).

the mitochondrial and ER fractions (at 48 h after infection), were treated with TBHP (75 μM) or diluent for 3 h. While this concentration of TBHP had no effect on annexin V staining in any treatment group at 24 h after infection (**Fig. 7A**) in RPTCs exposed to diluent (control) or scramble shRNA for 48 h, it caused a 2-fold increase in annexin V staining in RPTCs with decreased ER and mitochondrial iPLA$_2$γ expression (Fig. 7B). No increases in PI staining were detected in any treatment group at any time point (data not shown). In summary, RPTCs with decreased iPLA$_2$γ undergo apoptosis in the presence of a low concentration of the oxidant TBHP, whereas RPTCs with control levels of iPLA$_2$γ or a limited decrease in iPLA$_2$γ protein do not.

Nonlethal oxidative stress induces iPLA$_2$γ expression in RPTCs

Previous studies from our laboratory and the results of the current study demonstrate that iPLA$_2$γ is an important protective enzyme in RPTCs during oxidative stress. Accordingly, we investigated whether iPLA$_2$γ expression in RPTC ER and mitochondria is induced in the presence of nonlethal oxidant exposure. RPTCs were exposed to 50 μM TBHP or diluent for 24 h, and the expression of iPLA$_2$γ was measured by immunoblot analysis (**Fig. 8A**). These treatment conditions did not result in RPTC cell death, as confirmed by annexin V and PI staining (data not shown). Twenty-four hours after exposure to 50 μM TBHP, expression of iPLA$_2$γ was significantly induced (~30%) in both the ER and mitochondria of RPTCs (Fig. 8B).

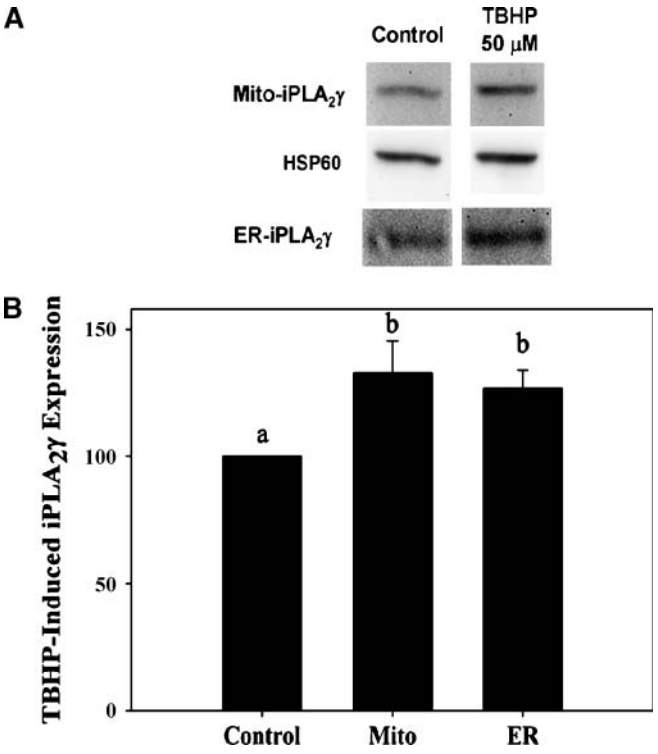

Fig. 8. Effects of nonlethal oxidative stress on iPLA$_2$γ expression in RPTCs. Control RPTCs were exposed to TBHP (50 μM) or diluent for 24 h and cells were harvested and fractionated into ER and mitochondrial fractions. iPLA$_2$γ expression was determined by immunoblot analysis (A) as described in Experimental Procedures. Data are expressed as means + SEM, percentage of control iPLA$_2$γ expression (determined by densitometry) (B). Means with different superscripts are significantly different from each other ($P < 0.05$, n = 4).

DISCUSSION

The development and use of an iPLA$_2$γ shRNA adenoviral vector in primary cultures of rabbit RPTCs enabled us to examine the role of this enzyme in cell physiology and in the setting of increased oxidative stress. Decreased expression of this enzyme in RPTCs caused an immediate and sustained increase in cellular lipid peroxidation. The increase in peroxidized lipids was followed by a decrease in mitochondrial function and eventually apoptotic cell death. Furthermore, knock-down of iPLA$_2$γ sensitized RPTCs to nonlethal concentrations of an oxidant. These results support the hypothesis that iPLA$_2$γ participates in the prevention of oxidation or repair of oxidized phospholipids and highlights the importance of this enzyme in mitochondrial and ER function.

After exposure of RPTCs to iPLA$_2$γ shRNA, expression of ER-iPLA$_2$γ decreased by 40% at 24 h. The finding that the 24 h level of mitochondrial iPLA$_2$γ expression was not different from the control level suggests that the rate of turnover of ER-iPLA$_2$γ is faster than mitochondrial iPLA$_2$γ in RPTCs. Furthermore, because cellular lipid peroxidation was significantly elevated at 24 h, we suggest that ER-iPLA$_2$γ is a vital component of the cellular lipid peroxidation repair pathway in RPTCs. At 48 and 72 h after iPLA$_2$γ shRNA exposure (when mitochondrial iPLA$_2$γ expression and activity were decreased by 30–60%), lipid peroxidation remained elevated but did not increase above the 24 h level. Thus, we hypothesize that cells with lipid peroxidation greater than the level observed in the 24 h iPLA$_2$γ knock-down group underwent cell death and detached from the culture dish.

In this model, we promoted a shift from the physiological condition to a pathological condition by decreasing iPLA$_2$γ activity through the introduction of shRNA for iPLA$_2$γ. During the first 48 h, phospholipid changes occurred in the ER and mitochondria, resulting in mitochondrial dysfunction. By 72 h, the cells with decreased iPLA$_2$γ could not withstand these phospholipid changes (oxidation, phospholipid substrate buildup, etc.) and began to die. Phospholipid changes were not measured once cell death began because of the difficulty in determining whether the phospholipid changes were the result of the loss of iPLA$_2$γ or were due to the cell death process.

With ESI-MS analysis of the phospholipids, we identified the most classes to be affected. Increased levels of these phospholipids suggested that the loss of iPLA$_2$γ led to changes in the cellular milieu that affected cellular activity.

The transience of these changes likely reflected time-dependent differences in the loss of iPLA$_2\gamma$ between the mitochondria and ER or compensatory changes that occurred over time when other PLA$_2$ activities possibly became affected.

The loss of iPLA$_2\gamma$ also resulted in an increase in substrate accumulation: saturated and unsaturated fatty acid-containing phospholipids. The accumulated unsaturated cellular phospholipids are potential targets of oxidative attack, leading to further damage. This hypothesis is supported by the TBARS data that showed that loss of iPLA$_2\gamma$ led to greater lipid peroxidation in RPTCs. In addition, changes in saturated fatty acid-containing phospholipids may affect membrane fluidity, affecting organelle functionality.

The effect of iPLA$_2\gamma$ shRNA on mitochondrial function was most likely the result of decreased mitochondrial iPLA$_2\gamma$ protein expression, as the loss of mitochondrial function was not observed until 48 h after infection when mitochondrial iPLA$_2\gamma$ expression and activity were decreased. The initial defect in mitochondrial function was identified at 48 h by determining the maximum capacity of the electron transport chain using the uncoupler FCCP. This stress test revealed a 25% decrease in electron transport capacity without a decrease in basal QO_2 or ATP levels. At 96 h, mitochondrial function was further decreased, as reflected by decreased basal QO_2 and decreased ATP. Because mitochondrial iPLA$_2\gamma$ is localized to the inner membrane (5), it is likely that the loss of mitochondrial iPLA$_2\gamma$ resulted in insufficient maintenance of the phospholipid composition or accumulation of oxidized phospholipids in the inner membrane, which, in turn disrupted electron transport. iPLA$_2\gamma$ may selectively cleave oxidized phospholipids, which are generated by reactive oxygen species during normal oxidative metabolism, in the inner mitochondrial membrane to preserve membrane integrity and prevent the impairment of complex III function (24). Alternatively, or additionally, iPLA$_2\gamma$ may be responsible for generating lysocardiolipin, which is reacylated during inner mitochondrial membrane remodeling, a critical process for the optimal function of complexes I, III, and IV of the electron transport chain (25, 26). In summary, the localization of iPLA$_2\gamma$ to the inner mitochondrial membrane, the importance of inner mitochondrial membrane phospholipids to the electron transport chain, and our observations that mitochondrial function decreased with decreased iPLA$_2\gamma$ suggest that iPLA$_2\gamma$ activity is required to maintain mitochondrial function.

The induced decrease in iPLA$_2\gamma$ expression resulted in elevated apoptosis, as measured by increased numbers of cells with condensed and fragmented nuclei and annexin V staining at 72 and 96 h. Apoptosis observed under these conditions may be the result of several mechanisms. Lipid peroxidation in the ER may have increased ER Ca^{2+} permeability, resulting in an elevated cytosolic free Ca^{2+} concentration that is known to induce apoptosis in this and other models (16, 27). Ca^{2+} accumulation by mitochondria may have initiated the mitochondrial permeability transition (MPT), a well-known signal for apoptosis (28). In addition, mitochondrial lipid peroxidation possibly initiated the MPT and caused the release of apoptotic mediators, including cytochrome *c* (29), or it may have led to an increase in Ca^{2+}-dependent PLA$_2$ activity. Finally, a lipid peroxidation end product, 4-hydroxynonenal, which reportedly induces apoptosis by modulating the activities of Jun and p38 kinases (30, 31), may have accumulated in RPTCs with decreased iPLA$_2\gamma$. In summary, several mechanisms may mediate apoptosis induced by decreased iPLA$_2\gamma$.

Upregulation of other lipid peroxidation repair enzymes and/or cellular antioxidants may compensate for the gradual decrease in iPLA$_2\gamma$ expression. One alternative pathway involves the L- and S-isoforms of phospholipid hydroperoxide glutathione peroxidase (32). Although phospholipid hydroperoxide glutathione peroxidase can directly reduce peroxidized phospholipids in membranes (33), its activity has been reported to be up to 500-fold less than that of cytosolic glutathione peroxidase (34). As mentioned above, the rate-limiting step in cytosolic glutathione peroxidase activity is PLA$_2$-mediated hydrolysis of the peroxidized fatty acid. A second potential lipid peroxidation repair enzyme, peroxiredoxin VI, is highly expressed in the lung (35). It is unknown at this time whether one or both of these pathways are functional in rabbit RPTCs. Upregulation of catalase, superoxide dismutase, or glutathione may also be consequences of iPLA$_2\gamma$ knock-down. In summary, upregulation of other antioxidant enzymes and molecules may have occurred to compensate for the gradual and prolonged decrease in iPLA$_2\gamma$.

In apparent contrast to a previous study in RPTCs demonstrating that pharmacologic inhibition of iPLA$_2\gamma$ deceases cisplatin-induced apoptosis (36), knock-down of iPLA$_2\gamma$ in this study resulted in RPTC apoptosis after oxidant exposure. In the cisplatin-induced RPTC apoptosis model, cell death is not mediated by oxidative stress but by DNA damage and iPLA$_2\gamma$-mediated caspase activation (36, 37). The mechanism by which iPLA$_2\gamma$ knock-down sensitizes RPTCs to oxidant-induced apoptosis has not been examined, but it may be the result of increased cytosolic Ca^{2+} due to ER lipid peroxidation and the effect of Ca^{2+} and lipid peroxidation on mitochondria (inducing MPT), as addressed above. Evidence for opposing roles of iPLA$_2\gamma$ in RPTCs after oxidant versus nonoxidant insults has accumulated in recent years. For example, in RPTCs and isolated RCM, iPLA$_2\gamma$ inhibition accelerates oxidant-induced lipid peroxidation, mitochondrial dysfunction, and cell death (4, 5). In contrast, iPLA$_2\gamma$ mediates cisplatin-induced RPTC apoptosis (36) and Ca^{2+}-induced MPT in RCM (38), demonstrating that RPTC iPLA$_2\gamma$ can be protective or detrimental in oxidant and nonoxidant stress, respectively.

Because all available data regarding the role of iPLA$_2\gamma$ in oxidant-induced lipid peroxidation, mitochondrial damage, and cell death suggest that iPLA$_2\gamma$ is part of the RPTC defense against oxidative stress, we hypothesized that its expression would be upregulated in the presence

of nonlethal oxidative stress. We confirmed this hypothesis. Additional studies are required to determine the mechanism by which iPLA$_2\gamma$ expression is increased by oxidative stress and whether iPLA$_2\gamma$ expression is induced by other sources of oxidative stress.

In conclusion, we demonstrate that selectively decreasing iPLA$_2\gamma$ expression and activity resulted in increased lipid peroxidation, impaired mitochondrial function, and ultimately apoptotic cell death in RPTCs. Exposure of RPTCs, with decreased expression of iPLA$_2\gamma$, to TBHP caused a 2-fold increase in apoptotic cell death, whereas no toxicity was observed in controls. These results are consistent with previous experiments in RPTCs and in isolated RCM showing that pharmacological inhibition of iPLA$_2\gamma$ increased lipid peroxidation, mitochondrial damage, and cell death induced by oxidants. Furthermore, the expression of iPLA$_2\gamma$ was increased in both ER and mitochondria as part of the response of RPTCs to oxidative stress. Collectively, these data suggest that iPLA$_2\gamma$ is a protective enzyme in the kidney under basal conditions and during oxidative stress.

The authors thank Prof. Yefim Manevich (Medical University of South Carolina) for his advice and critical reading of the manuscript.

REFERENCES

1. Schaloske, R. H., and E. A. Dennis. 2006. The phospholipase A2 superfamily and its group numbering system. *Biochim. Biophys. Acta.* **1761:** 1246–1259.
2. Balsinde, J., M. V. Winstead, and E. A. Dennis. 2002. Phospholipase A(2) regulation of arachidonic acid mobilization. *FEBS Lett.* **531:** 2–6.
3. Balsinde, J., I. D. Bianco, E. J. Ackermann, K. Conde-Frieboes, and E. A. Dennis. 1995. Inhibition of calcium-independent phospholipase A2 prevents arachidonic acid incorporation and phospholipid remodeling in P388D1 macrophages. *Proc. Natl. Acad. Sci. USA.* **92:** 8527–8531.
4. Cummings, B. S., J. McHowat, and R. G. Schnellmann. 2002. Role of an endoplasmic reticulum Ca(2+)-independent phospholipase A(2) in oxidant-induced renal cell death. *Am. J. Physiol. Renal Physiol.* **283:** F492–F498.
5. Kinsey, G. R., J. McHowat, C. S. Beckett, and R. G. Schnellmann. 2007. Identification of calcium-independent phospholipase A2 {gamma} in mitochondria and its role in mitochondrial oxidative stress. *Am. J. Physiol. Renal Physiol.* **292:** F853–F860.
6. Seleznev, K., C. Zhao, X. H. Zhang, K. Song, and Z. A. Ma. 2006. Calcium-independent phospholipase A2 localizes in and protects mitochondria during apoptotic induction by staurosporine. *J. Biol. Chem.* **281:** 22275–22288.
7. van Kuijk, F. J. G. M., A. Sevanian, G. J. Handelman, and E. A. Dratz. 1987. A new role for phospholipase A2: protection of membranes from lipid peroxidation damage. *Trends Biochem. Sci.* **12:** 31–34.
8. Lands, W. E. 1965. Lipid metabolism. *Annu. Rev. Biochem.* **34:** 313–346.
9. Sevanian, A., S. F. Muakkassah-Kelly, and S. Montestruque. 1983. The influence of phospholipase A2 and glutathione peroxidase on the elimination of membrane lipid peroxides. *Arch. Biochem. Biophys.* **223:** 441–452.
10. van Kuijk, F. J., G. J. Handelman, and E. A. Dratz. 1985. Consecutive action of phospholipase A2 and glutathione peroxidase is required for reduction of phospholipid hydroperoxides and provides a convenient method to determine peroxide values in membranes. *J. Free Radic. Biol. Med.* **1:** 421–427.
11. Salgo, M. G., F. P. Corongiu, and A. Sevanian. 1992. Peroxidation and phospholipase A2 hydrolytic susceptibility of liposomes consisting of mixed species of phosphatidylcholine and phosphatidylethanolamine. *Biochim. Biophys. Acta.* **1127:** 131–140.
12. Sevanian, A., and E. Kim. 1985. Phospholipase A2 dependent release of fatty acids from peroxidized membranes. *J. Free Radic. Biol. Med.* **1:** 263–271.
13. Kinsey, G. R., B. S. Cummings, C. S. Beckett, G. Saavedra, W. Zhang, J. McHowat, and R. G. Schnellmann. 2005. Identification and distribution of endoplasmic reticulum iPLA2. *Biochem. Biophys. Res. Commun.* **327:** 287–293.
14. Rasbach, K. A., and R. G. Schnellmann. 2007. Signaling of mitochondrial biogenesis following oxidant injury. *J. Biol. Chem.* **282:** 2355–2362.
15. Nowak, G., and R. G. Schnellmann. 1996. L-Ascorbic acid regulates growth and metabolism of renal cells: improvements in cell culture. *Am. J. Physiol.* **271:** C2072–C2080.
16. Cummings, B. S., G. R. Kinsey, L. J. Bolchoz, and R. G. Schnellmann. 2004. Identification of caspase-independent apoptosis in epithelial and cancer cells. *J. Pharmacol. Exp. Ther.* **310:** 126–134.
17. Schnellmann, R. G. 1994. Measurement of oxygen consumption. *In* Methods in Toxicology. C. A. Tyson and J. M. Frazier, editors. Academic Press, New York. 128–139
18. Rasbach, K. A., and R. G. Schnellmann. 2007. PGC-1alpha overexpression promotes recovery from mitochondrial dysfunction and cell injury. *Biochem. Biophys. Res. Commun.* **355:** 734–739.
19. Bligh, E. G., and W. J. Dyer. 1959. A rapid method of total lipid extraction and purification. *Can. J. Med. Sci.* **37:** 911–917.
20. Zhang, L., B. L. Peterson, and B. S. Cummings. 2005. The effect of inhibition of Ca2+-independent phospholipase A2 on chemotherapeutic-induced death and phospholipid profiles in renal cells. *Biochem. Pharmacol.* **70:** 1697–1706.
21. Zhou, X., and G. Arthur. 1992. Improved procedures for the determination of lipid phosphorus by malachite green. *J. Lipid Res.* **33:** 1233–1236.
22. Forrester, J. S., S. B. Milne, P. T. Ivanova, and H. A. Brown. 2004. Computation lipidomics: a multiplexed analysis of dynamic changes in membrane lipid composition during signal transduction. *Mol. Pharm.* **65:** 813–821.
23. Ivanova, P. T., S. B. Milne, J. S. Forrester, and H. A. Brown. 2004. Lipid arrays: new tools in the understanding of membrane dynamics and lipid signaling. *Mol. Interv.* **4:** 86–96.
24. Petrosillo, G., F. M. Ruggiero, N. Di Venosa, and G. Paradies. 2003. Decreased complex III activity in mitochondria isolated from rat heart subjected to ischemia and reperfusion: role of reactive oxygen species and cardiolipin. *FASEB J.* **17:** 714–716.
25. Hauff, K. D., and G. M. Hatch. 2006. Cardiolipin metabolism and Barth syndrome. *Prog. Lipid Res.* **45:** 91–101.
26. McKenzie, M., M. Lazarou, D. R. Thorburn, and M. T. Ryan. 2006. Mitochondrial respiratory chain supercomplexes are destabilized in Barth syndrome patients. *J. Mol. Biol.* **361:** 462–469.
27. Penzo, D., V. Petronilli, A. Angelin, C. Cusan, R. Colonna, L. Scorrano, F. Pagano, M. Prato, F. Di Lisa, and P. Bernardi. 2004. Arachidonic acid released by phospholipase A(2) activation triggers Ca(2+)-dependent apoptosis through the mitochondrial pathway. *J. Biol. Chem.* **279:** 25219–25225.
28. Lemasters, J. J., T. Qian, L. He, J. S. Kim, S. P. Elmore, W. E. Cascio, and D. A. Brenner. 2002. Role of mitochondrial inner membrane permeabilization in necrotic cell death, apoptosis, and autophagy. *Antioxid. Redox Signal.* **4:** 769–781.
29. Petrosillo, G., G. Casanova, M. Matera, F. M. Ruggiero, and G. Paradies. 2006. Interaction of peroxidized cardiolipin with rat-heart mitochondrial membranes: induction of permeability transition and cytochrome c release. *FEBS Lett.* **580:** 6311–6316.
30. Awasthi, Y. C., R. Sharma, J. Z. Cheng, Y. Yang, A. Sharma, S. S. Singhal, and S. Awasthi. 2003. Role of 4-hydroxynonenal in stress-mediated apoptosis signaling. *Mol. Aspects Med.* **24:** 219–230.
31. Kutuk, O., G. Poli, and H. Basaga. 2006. Resveratrol protects against 4-hydroxynonenal-induced apoptosis by blocking JNK and c-JUN/AP-1 signaling. *Toxicol. Sci.* **90:** 120–132.
32. Arai, M., H. Imai, T. Koumura, M. Yoshida, K. Emoto, M. Umeda, N. Chiba, and Y. Nakagawa. 1999. Mitochondrial phospholipid hydroperoxide glutathione peroxidase plays a major

role in preventing oxidative injury to cells. *J. Biol. Chem.* **274:** 4924–4933.
33. Ursini, F., M. Maiorino, A. Roveri, L. Ferri, and C. Gregolin. 1982. Purification from pig liver of a protein which protects liposomes and biomembranes from peroxidative degradation and exhibits glutathione peroxidase activity on phosphatidylcholine hydroperoxides. *Biochim. Biophys. Acta.* **710:** 197–211.
34. Zhang, L. P., M. Maiorino, A. Roveri, and F. Ursini. 1989. Phospholipid hydroperoxide glutathione peroxidase: specific activity in tissues of rats of different age and comparison with other glutathione peroxidases. *Biochim. Biophys. Acta.* **1006:** 140–143.
35. Manevich, Y., and A. B. Fisher. 2005. Peroxiredoxin 6, a 1-Cys peroxiredoxin, functions in antioxidant defense and lung phospholipid metabolism. *Free Radic. Biol. Med.* **38:** 1422–1432.
36. Cummings, B. S., J. McHowat, and R. G. Schnellmann. 2004. Role of an endoplasmic reticulum Ca2+-independent phospholipase A2 in cisplatin-induced renal cell apoptosis. *J. Pharmacol. Exp. Ther.* **308:** 921–928.
37. Cummings, B. S., and R. G. Schnellmann. 2002. Cisplatin-induced renal cell apoptosis: caspase 3-dependent and -independent pathways. *J. Pharmacol. Exp. Ther.* **302:** 8–17.
38. Kinsey, G. R., J. McHowat, K. S. Patrick, and R. G. Schnellmann. 2007. Role of Ca2+-independent phospholipase A2{gamma} in Ca2+-induced mitochondrial permeability transition. *J. Pharmacol. Exp. Ther.* **321:** 707–715.